Dalton Transactions

ROYAL SOCIETY OF CHEMISTRY

PERSPECTIVE

View Article Online
View Journal

Cite this: DOI: 10.1039/d6dt00293e

Stabilizing the E≡N triple bonds in pnictogen mononitrides

Aswin Chandran, Simon Edin, Mattias Tan and Anders Reinholdt *

The viability of a main-group triple bond depends critically on the strength of its π-manifold. Among the 15 possible diatomic homo- and interpnictogens, E≡E′, (E, E′ = group 15 element), the N≡N linkage of dinitrogen stands out as one of the strongest triple bonds that exists, whereas the heavier pnictogens form thermodynamically unstable triple bond motifs that either decompose to single-bonded oligomers or extrude N_2, under standard conditions. Considering the fundamentally simple chemistry of a diatomic molecule, coupled with the enticing synthetic challenge of accessing any other E≡E′ dipnictogen than N_2, we here survey the chemistry of the mononitride family, E≡N (E = P, As, Sb, Bi). We describe how these unusual bonding motifs were first observed as transient species in the gas phase, later isolated in cryogenic noble-gas matrix experiments, and recently have become the subject of synthetic studies in solution. We delineate strategies to tame the highly reactive E≡N motifs by incorporating them into adducts with organic fragments or transition metal nodes, enabling studies of their reaction chemistry under controlled conditions. These efforts have opened fascinating perspectives in pnictogen multiple-bond reactivity, spanning radical and closed-shell transformations, electrophilic as well as nucleophilic reactivity of the E≡N fragments, oxidative addition, oligomerization, cyclization, inorganic aromaticity, and even E≡N group transfer. Finally, we identify topics in the triple-bond chemistry of pnictogen mononitrides that remain ambiguous or poorly explored, pointing toward future directions in the field.

Received 4th February 2026,
Accepted 5th March 2026

DOI: 10.1039/d6dt00293e

rsc.li/dalton

Introduction

Together with alkynes, dinitrogen (N≡N) is likely one of the first triple-bonded molecules that a chemistry student encounters, placing it centrally in our conceptualization of multiple

Department of Chemistry, Centre for Analysis and Synthesis, Lund University, Naturvetarvägen 22, 22100 Lund, Sweden. E-mail: anders.reinholdt@chem.lu.se

Aswin Chandran

Aswin Chandran was born in Kerala, India. He received his M. Sc. from NIT Tiruchirappalli (2020), with research on low-coordinate lead complexes at LHFA-CNRS, Toulouse, under Dr Tsuyoshi Kato. He obtained his Ph.D. (2020–2024) through an MSCA ITN European Joint Doctorate between the University of York (Prof. Jason Lynam and Dr John Slattery) and the University of Toulouse III Paul Sabatier (Dr Mary Grellier). His doctoral research focused on silicon and germanium coordination at ruthenium centers for catalysis. In 2024, he joined Lund University as a postdoctoral researcher with Dr Anders Reinholdt, focusing on early transition metal phosphide and low-valent complexes.

Simon Edin

Simon Edin was born in Luleå, Sweden. He obtained his B.Sc. in Chemistry (2020) from Lund University and completed his M. Sc. thesis (2022) under the guidance of Prof. Kenneth Wärnmark, working on the synthesis of hydrogen bonding monomers for controlled self-assembly. In 2023, Simon joined the research group of Anders Reinholdt at Lund University to pursue his Ph.D., with an interest in pnictogen mononitrides.

bonds, and chemical bonding theory. The N≡N linkage (945 kJ mol^{-1}) is essentially the second-strongest triple bond that exists; it is chemically inert, and thermodynamically very stable. These fundamental properties of N_2 are by no means confined to being academic curiosities, considering that an estimated 1–2% of the World's annual energy consumption goes into running the Haber–Bosch process,[1] splitting the N≡N triple bond, and forming ammonia and a wealth of useful nitrogen-containing products downstream therefrom. In comparison to N_2, the heavier group 15 elements form drastically less stable triple bonds, and the chemistry of such diatomic interpnictogen functionalities remains very limited, reflecting the short-lived and highly reactive character of these molecules in their free state. In recent years, this instability has prompted researchers to design molecular scaffolds – spanning unsaturated organics over transition metal architectures – to stabilize the triple-bonded diatomics as well-defined adducts. These strategies have opened explorations of the chemistry of simple pnictogen molecules under controlled conditions. Exotic chemistry of these units has begun to emerge, ranging from unique binding modes, photochemical transformations, coordination chemistry, solution transfer reactions, open-shell systems, and inorganic aromaticity. The following paragraphs lay out the chemistry of diatomic, triple-bonded molecules composed of nitrogen and the heavier pnictogens, starting from their history of isolation, followed by more recent endeavors to control their chemistry.

Free E≡N diatomics

A diatomic group defines the transition from atom to molecule and conceptually sets the boundaries for chemical bonding theory. Two-atom fragments such as $C{\equiv}N^-$, N≡N, and $N{\equiv}O^+$ represent some of the strongest triple bonds that exist, and occur widely as ligands in transition metal chemistry. However, when introducing heavier p-block elements into analogous E≡E′ motifs, the resulting triple bonds become dramatically less stable with respect to oligomeric, single-bonded decomposition products. Virtually all such heavy-element diatomics have a transient existence, and studies of their vulnerable triple bonds have largely been restricted to extreme conditions, such as high-vacuum and/or cryogenic matrix setups. Despite these challenges, methods to control the reactivity of short-lived, triple-bonded diatomics could provide unique insight into orbitally mismatched bonds and unlock fundamental reactivity of species that otherwise only have a speculative existence.

To contextualize efforts to study the chemistry of E≡N diatomic adducts under controlled conditions, and in solution, the following sections outline important milestones in the chemistry of the free diatomic E≡N molecules.

Discovery of free E≡N diatomics

By the time that nitrogen was first isolated (Daniel Rutherford, 1772, significant contemporaneous contributions from Carl Wilhelm Scheele, Henry Cavendish, and Joseph Priestley),[2,3] all the heavier pnictogens had been known for more than a hundred years, with phosphorus marking the penultimate discovery of a group 15 element (Hennig Brandt, 1669). In contrast to the heavier elements, which were isolated as single-bonded molecules, polymeric substances, or metals, their lighter congener poses a strikingly different bonding scenario, consisting of two atoms connected by a triple bond.

Based on the chemical similarity between group 15 elements, it is natural to inquire into the possible existence of diatomic motifs consisting of a heavy pnictogen with a triple bond to nitrogen (E≡N). All the heavier pnictogens, however, are indefinitely stable under 1 bar N_2 at room temperature, calling upon sophisticated synthetic strategies to incorporate these elements in triple-bonded motifs. With the advent of

Mattias Tan

Mattias Tan studied at Lund University (Sweden) where he received his M.Sc. degree in the field of inorganic chemistry with focus on catalysis with bio-organic molecules. He now works as a doctoral candidate at Lund University where he joined the Anders Reinholdt research group. His focus is on the field of small molecule activation with group 15 elements stabilized by transition metals, to enable effective synthesis of exotic molecules.

Anders Reinholdt

Anders Reinholdt was born in Odense, Denmark. He obtained his Ph.D. (2018) from the University of Copenhagen, under the guidance of Prof. Jesper Bendix, working on the reactivity and electronic structure of ruthenium carbide complexes. He subsequently carried out postdoctoral studies with Prof. Daniel J. Mindiola at the University of Pennsylvania (2019–2021), working on low-valent titanium complexes in low-coordinate geometries. In 2022, Anders started his independent career at Lund University where his research group focuses on the synthesis, reactivity, mechanistic aspects, and electronic structure of main-group and transition metal multiple-bonded systems.

microwave spectroscopy, it became possible to gain highly precise structural information on small molecules in the gas phase, based on analysis of their rotational spectra. This enabled authentication of P≡N (1933),[4] As≡N (1934),[5] and Sb≡N (1940)[6] in short order, whereas Bi≡N completed the series only in 1993.[7] Fascinatingly, in 1987, P≡N was detected as a surprisingly abundant molecule in interstellar space,[8,9] and it has since been observed in outgassing vapor from a comet,[10] and even at the edge of the Galaxy.[11] Fig. 1 summarizes the year of discovery, as well as key physical parameters (bond dissociation enthalpy, fundamental stretching vibration, equilibrium bond distance) for E≡N molecules in the gas phase.

Synthetic strategies toward free E≡N diatomics

Considering their transient nature, free E≡N molecules can virtually only be generated in dilute gas-phase mixtures at high temperature. Under such conditions, the combined effects of infrequent collisions along with the higher entropy of diatomic molecules relative to polyatomic alternatives, allow for spectroscopic detection of these short-lived and highly reactive species. In 1933, Herzberg synthesized P≡N by letting a discharge through a tube containing nitrogen and phosphorus vapor, leading to recombination of the elements and formation of the interpnictogen (Fig. 2).[4] In 1977, Timms showed how phosphorus(v) nitride thermally decomposes (800–900 °C) to form gaseous P≡N, which was trapped and spectroscopically characterized in a matrix of solid Kr (10 K).[16] Weak interactions with the noble gas matrix shifted the fundamental P≡N stretching frequency from 1337 (gas phase) to 1323 cm^{-1} (matrix); the latter band shifted to 1293 cm^{-1} for the $^{31}P\equiv{}^{15}N$ isotopologue, in agreement with the expected value for a harmonic oscillator (1292 cm^{-1}). Upon heating the matrix-isolated P≡N molecules to 25 K, their extreme reactivity led to bands from a new species, deduced to be *cyclo*-triphosphazene (P_3N_3).[16–18] In a follow-up study, Timms found evidence that P≡N might serve as a ligand, when condensed into a cryogenic Kr matrix together with metal atom vapor (Cu, Ag, Au, at 10 K).[19] In 1989, Schnöckel reported a third route to P≡N; the interpnictogen was generated by passing $[N_3P_3Cl_6]$ vapor over silver at 1300 K, resulting in dehalogenation and retro-cyclization of the phosphazene.[20] Finally, in 2023, Mardyukov utilized the redox interconvertability of catecholate/*ortho*-benzoquinone to access P≡N.[21] When kept in an Ar matrix (10 K), the azidophosphine, $[(C_6H_4O_2)P(N_3)]$, was photolyzed at

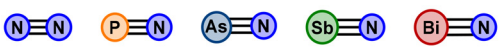

	N≡N	P≡N	As≡N	Sb≡N	Bi≡N
discovery	**1772**	**1933**	**1934**	**1940**	**1993**
BDE / kJ mol^{-1}	945[a]	614[a]	485[b]	377[c]	284[b]
$\tilde{\nu}$ / cm^{-1}	2359[a]	1337[a]	1069[a]	865[c]	737[d]
d / Å	1.097685[a]	1.490866[a]	1.61843[a]	1.8352[c]	1.93491[d]

Fig. 1 Structure of the group 15 E≡N diatomics (E = N–Bi), along with discovery year, bond dissociation enthalpy, fundamental stretching vibration, and bond distance. Data taken from *a*,[12] *b*,[13] *c*,[14] *d*.[15]

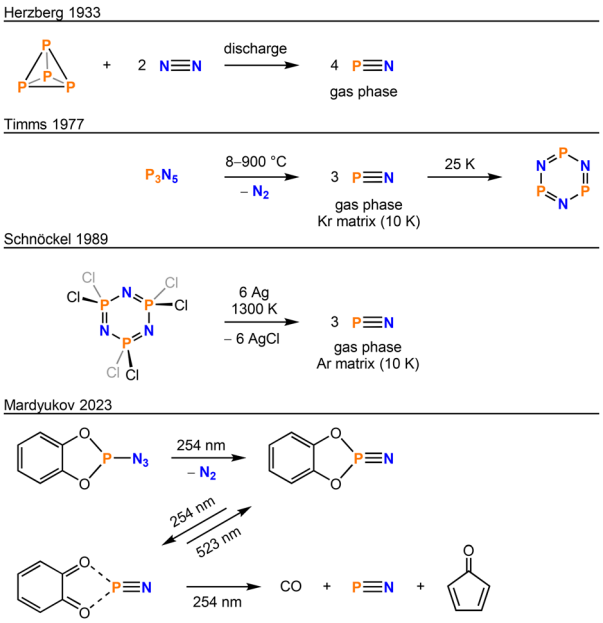

Fig. 2 Synthetic routes to free P≡N molecule.

254 nm, to form N_2 along with a $[(C_6H_4O_2)P\equiv N]$ species. This organic adduct of P≡N possesses two valence forms, involving either a catecholate dianion or a neutral *ortho*-benzoquinone. Interestingly, P≡N was ultimately released photolytically from the $[(C_6H_4O_2)P\equiv N]$ species, but the release was not accompanied by simultaneous formation of *ortho*-benzoquinone, but instead CO and cyclopentadienone were observed as a result of a ring-contraction process.

While it has been possible to isolate P≡N under cryogenic conditions in noble gas matrices, these protective measures have mired its reactivity. However, in recent years, Zeng has shown how mono- and dihydrogenated products can be accessed through carefully adjusted flash-pyrolysis followed by matrix isolation. For example, the isocyanatophosphine, $^tBu_2P(NCO)$, eliminates 2-methylpropene and *tert*-butyl radical, to form a HP–NCO• intermediate. Subsequent photolysis produces the radical tautomers, HPN• and PNH•, as weak CO complexes (3–10 K).[22] In a related fashion, flash-pyrolysis of the aminophosphine, $^tBu_2PNH_2$, followed by matrix isolation (10 K), provides access to the *cis* and *trans* isomers of iminophosphane, HP═NH, as well as iminophosphinidene, $P{=}NH_2$ (Fig. 3).[23]

Shortly after the first synthesis of P≡N, the synthesis of As≡N was carried out by analogy to its lighter congener (Fig. 4). In 1934, Spinks subjected metallic arsenic and gaseous N_2 to an electrical discharge inside a tube, enabling spectroscopic identification of the As≡N molecule from 30 rotational bands.[5] Another gas-phase synthesis of As≡N was reported by Coombe in 1988.[24] By combining a vapor of arsenic atoms (in their ground quartet state) with gaseous nitridyl radical, N_3•, the diatomic arsenic mononitride molecule was generated upon loss of dinitrogen. This high-energy synthesis prepared the As≡N molecule in an electronically

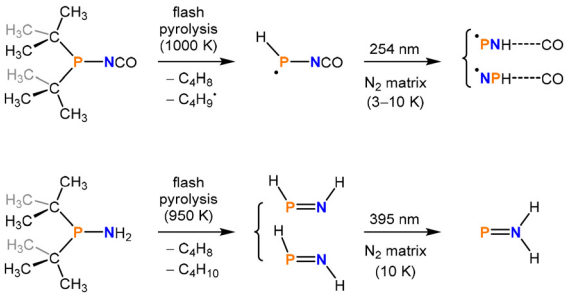

Fig. 3 Flash pyrolysis of bis(*tert*-butyl) phosphines, followed by matrix isolation, to isolate PNH•/NPH• as CO complexes, as well as *cis*-HP═NH, *trans*-HP═NH, and P═NH_2.

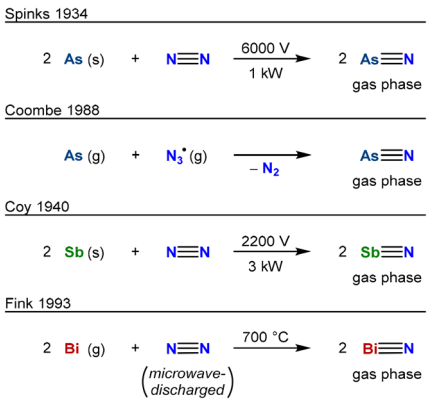

Fig. 4 Synthetic routes to free As≡N, Sb≡N, and Bi≡N molecules in the gas phase.

excited state, likely to be a triplet. Quite interestingly, a polymeric, cubic phase of composition [AsN] was recently generated under high-pressure conditions in a diamond anvil cell (30–40 GPa).[25,26] In the case of antimony, the gas-phase synthesis of Sb≡N was reported by Coy in 1940.[6] By subjecting metallic antimony and nitrogen gas to an electric discharge, the diatomic Sb≡N molecule could be identified from its rotational lines. Several later works have accessed Sb≡N through similar strategies, *i.e.* in high-energy reactions between N_2 and antimony.[14,27,28] Considering the timeline in the gas-phase generation of P≡N, As≡N, and Sb≡N (1933–1940), it is striking that Bi≡N was not reported until 1993. By subjecting bismuth vapor to microwave-discharged N_2, Fink generated the transient Bi≡N molecule and unequivocally confirmed its existence based on the spectral differences between the Bi≡^{14}N and Bi≡^{15}N isotopologues.[7] More recently, a polymeric [BiN] phase was prepared in a high-pressure, high-temperature synthesis, in which bismuth and dinitrogen confined inside a diamond-anvil cell were heated using a near-infrared laser.[29,30]

Bonding in free E≡N diatomics

To appreciate the underlying thermodynamic parameters that determine the stability of a diatomic E≡N system, it is instructive to consider the enthalpy change for decomposition of P≡P, P≡N, and As≡N into their constituent elements, in standard state (Fig. 5). Starting from P≡P, it is immediately apparent that its triple bond enthalpy only moderately exceeds the sum of two P–P single bonds, and dimerization into $\frac{1}{2}$ eq. P_4 is energetically preferred [–137 kJ mol^{-1}]. In other words, when the 3p orbitals of phosphorus overlap, they form π-bonds that are weak in comparison to the corresponding σ-bonds. Turning to P≡N, this interpnictogen is thermodynamically more unstable [–173 kJ mol^{-1}] than P≡P, even though its triple bond is stronger. While it might be tempting to attribute the instability of P≡N (relative to P≡P) to the covalent mismatch between the compact 2p orbitals of nitrogen and the more diffuse 3p valence orbitals of phosphorus, the trends in bond enthalpies suggest a significant ionic component to actually reinforce bonding in P≡N. But in terms of overall stability with respect to its constituent elements, this gain in bond strength for P≡N is entirely outweighed by the very strong triple bond in N_2. Seen in a wider perspective, the high thermodynamic stability of N_2 renders almost any binary nitride in the Periodic Table metastable; the existence of such phases therefore relies on sufficiently high kinetic barriers to prevent decomposition.[31–33] Nonetheless, the idea that orbital-mismatch decreases the stability of interpnictogens is not without merit. When considering As≡N, its triple bond is more than 100 kJ mol^{-1} weaker than that of P≡N, whereas As–As and P–P single bond enthalpies are similar in magnitude. This results in a drastically lowered enthalpic stability of As≡N with respect to the elements, and for similar reasons, Sb≡N and Bi≡N are even less stable. Not surprisingly, the following sections will demonstrate that there is a growing number of P≡N derivatives, very few As≡N analogs, and virtually no Sb≡N or Bi≡N fragments isolated in stable molecular architectures.

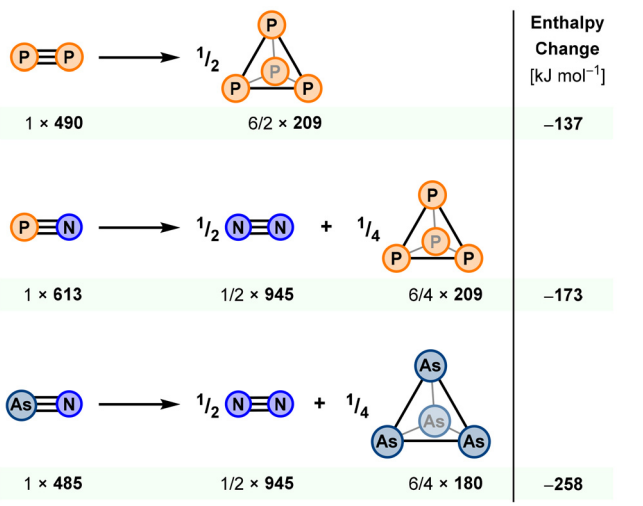

Fig. 5 Schematic illustration of enthalpic changes for conversion of P≡P, P≡N, and As≡N into their constituent elements.

Bond dissociation enthalpy data show that all E≡N molecules are unstable relative to their constituent elements (E = P–Bi), when entropic contributions are discounted. The formation of E–E σ-bonds and a very strong N≡N triple bond provides the driving force for decomposition. Given sufficient thermal energy, entropy will favor diatomics over larger systems such as P_4 or As_4,[34] explaining why E≡N molecules can be generated and spectroscopically observed at high temperatures in the gas phase. However, dilute gas-phase mixtures are not well suited, if at all, for generation of synthetically reasonable amounts of material for reactivity studies. On the other hand, if the E≡N diatomics were bound to a stabilizing fragment, the resulting adduct could be used to conduct reactions of these unusual triple bonds under controlled conditions, and in larger quantities. The following sections outline progress made in the study of such rare main-group motifs.

E≡N diatomics stabilized by organic fragments

A range of organic fragments have been deployed for the stabilization of E≡N diatomics. P≡N is reasonably well represented, and to a more limited extent also As≡N. On the other hand, organic derivatives of Sb≡N and Bi≡N remain to be crystallographically characterized. Overall, the following paragraphs show that derivatives of P≡N and As≡N are often stabilized by unsaturated organic groups (aryl, carbene, arene, alkene), which possess a π-electronic system suitable to interact with the π-manifold of the diatomic interpnictogen.

Aryl-stabilized P≡N derivatives

The very bulky supermesityl group (Mes* = 2,4,6-^{t}Bu$_3$C$_6$H$_2$) has been used to stabilize P≡N as a one-coordinate and cationic fragment, and a wide range of studies have been carried out on this system. Thus, the first structurally authenticated E≡N adduct was reported by Niecke in 1988, starting from the aniline, Mes*–NH_2. Treatment with PCl_3 and Et_3N initially generated an iminophosphine, [Mes*–N=PCl], which could subsequently undergo halide abstraction using $AlCl_3$ in toluene to form [Mes*–N≡P][$AlCl_4$] as a toluene-solvated salt (Fig. 6).[35] It should be noted that the chemistry of the intermediate, [Mes*–N=PCl], has been extensively explored;[36–48] in the context of interpnictogen triple bonds, one of the most notable conversions is Cummins' coupling of [Mes*–N=PCl] with a niobium arsenide moiety to form an {As=P=N–Mes*} ligand, capable of extruding a diatomic As≡P group.[49]

In a related fashion to the synthesis of [Mes*–N≡P]$^+$, Schulz later showed how the bis(trimethylsilyl)amido substituted chlorophosphine, [$(Me_3Si)_2$N–PCl_2] underwent chloride abstraction with $GaCl_3$ at −70 °C to form a [$(Me_3Si)_2$N=PCl][$GaCl_4$] salt (Fig. 7). Warming this compound to room temperature resulted in elimination of Me_3SiCl and formation of a silylated species, [Me_3Si–N≡P][$GaCl_4$], which could be spectroscopically observed.[50]

Interestingly, Burford found that when treating [Mes*–N=PCl] with $GaCl_3$ (instead of $AlCl_3$), but still using toluene as solvent, this reaction generated a salt, [Mes*–N≡P(toluene)][$GaCl_4$], with a close contact between phosphorus and the arene, suggesting the [Mes*–N≡P]$^+$ cation to be Lewis acidic (Fig. 8).[51] Similar adduct types have been reported for arenes such as benzene and mesitylene.[52] It should be noted that a related solid-state packing can be observed in the [$AlCl_4$]$^-$ salt of [Mes*–N≡P]$^+$, but this system exhibits a larger separation between phosphorus and the arene.

Extensive studies by Burford showed how the Lewis acidity of the [Mes*–N≡P]$^+$ cation enables coupling with main-group bases, including an N-heterocyclic carbene,[53] pyridines,[54] bipyridine,[55] polyamines,[56] PPh_3,[57] and chalcogenoureas.[58] The resulting [Mes*–N≡P–L][SO_3CF_3] motifs feature two-, three-, and four-coordinate phosphorus, involving hypercoordinated P^{III} centers (Fig. 9).

Considering that the positive charge in [Mes*–N≡P]$^+$ imparts this group with π-acceptor character, this triple-bonded system has been incorporated into various electron-rich metal complexes (Fig. 10). Niecke demonstrated how K[$FeCp^*(CO)_2$] and [Mes*–N=PCl] would eliminate KCl to form a Fe^{II} derivative, [Mes*–N=P–$FeCp^*(CO)_2$]. The bimetallic complex displays a zig-zag geometry for the {Mes*–N=P–Fe} core, indicating that an anionic resonance contributor for the ligand, [Mes*–N=P]$^-$, characterizes this 18-electron system.[59]

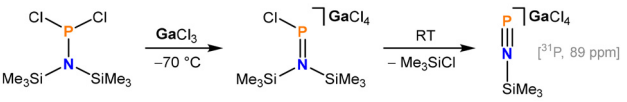

Fig. 7 Formation of a silyl-protected P≡N group.

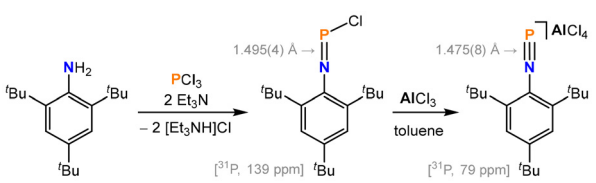

Fig. 6 Synthesis of [Mes*–N≡P][$AlCl_4$] upon halide abstraction from [Mes*–N=PCl] using $AlCl_3$.

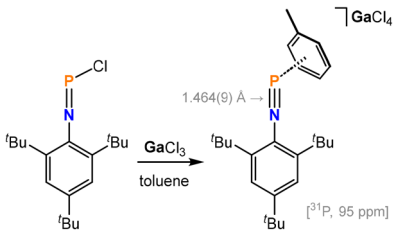

Fig. 8 Synthesis of [Mes*–N≡P(toluene)][$GaCl_4$] upon halide abstraction with $GaCl_3$.

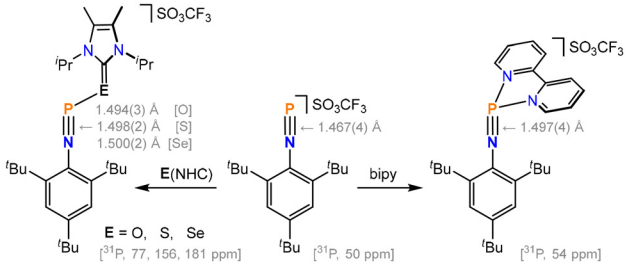

Fig. 9 Reactivity of [Mes*–N═P][SO_3CF_3] toward Lewis bases.

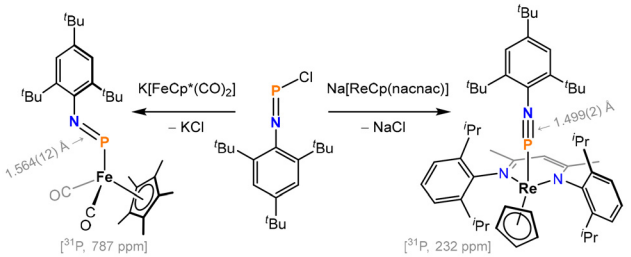

Fig. 10 Metallation of [Mes*–N═PCl] leading to [Mes*–N═P]$^-$ and [Mes*–N═P]$^+$ ligand systems.

Such a bonding geometry indicates the P≡N fragment to be a quite strong π-backbonding ligand, but it should also be noted that an alternative linear geometry for a [Mes*–N≡P]$^+$ ligand would have necessitated a 20-electron Fe^0 complex. More recently, Arnold found that the rhenium precursor Na[ReCp(nacnac)] reacts with [Mes*–N═PCl] to form a linearly coordinated, 18-electron [Mes*–N≡P–ReCp(nacnac)] complex.[60]

Another significant reaction mode is that the triflate, [Mes*–N≡P][SO_3CF_3], crystallizes in both monomeric[61] and dimeric[62] modifications (Fig. 11). The dimeric form contains a central {P_2N_2} fragment but dissociates to regenerate the monomeric form in solution. The reversible self-coupling suggests that the P≡N linkage in the cationic monomer is similar in strength compared to P–N single bonds in the dimer, showcasing the vulnerability of the P≡N π-bonds.

When the iminophosphine, [Mes*–N═PCl], is chlorinated, either using Cl_2, PCl_5, or $PhICl_2$, a hypervalent phosphorus(v) compound, [Mes*–N≡PCl_3], forms, which represents an imido

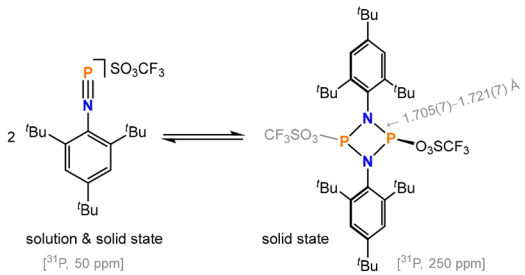

Fig. 11 Monomeric and dimeric forms of [Mes*–N≡P][SO_3CF_3].

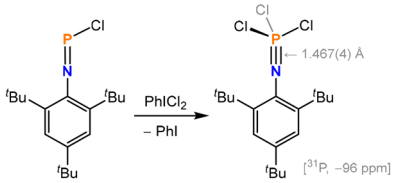

Fig. 12 Oxidation of [Mes*–N═PCl] with $PhICl_2$ to form [Mes*–N≡PCl_3].

analog of phosphoryl chloride (Fig. 12).[63,64] The halogenation chemistry can also be extended to encompass the tribromo and triiodo derivatives, [Mes*–N≡PBr_3] and [Mes*–N≡PI_3]. In line with a triple bond formulation, [Mes*–N≡PCl_3] possesses a very short P≡N distance, which is about 2% shorter than the corresponding bond distance in the free P≡N molecule.

The [Mes*–N≡P]$^+$ platform can also be used for [3 + 2] cyclization reactivity to form unusual inorganic heterocycles. Niecke showed how [Mes*–N≡P][$AlCl_4$] reacts with alkyl azides, ^{t}BuN$_3$ or Et_3CN_3, to form disubstituted tetrazaphosphole motifs, such as [Mes*(N_4P)CEt_3][$AlCl_4$] (Fig. 13).[65] In a related manner, Schulz later demonstrated how [Mes*–N═PCl] reacts with $GaCl_3$ and Me_3SiN_3 (which serves as both halide abstractor and azide source), forming the $GaCl_3$ adduct, [Mes*(N_4P)$GaCl_3$].[66]

Recently, Tan showed how a very bulky aryl amine, possessing flanking spirofluorene motifs as sterically protective groups, could be deprotonated with ^{n}BuLi, followed by reaction with PCl_3 and Et_3N to form an [Ar–N═PCl] motif (Fig. 14).[67] Significantly, the flanking spirofluorene groups completely suppress any tendency for the P═N double bonded motif to dimerize (known reaction mode in both Mes* [Fig. 11] and terphenyl-based systems[68]). Reduction of the [Ar–N═PCl] motif with KC_8 led to a stable iminophosphinyl radical, [Ar–N═P]$^\bullet$, which represents a molecular analog of the one-electron reduced radical anion of phosphorus mononitride, [P═N]$^{\bullet-}$. It should further be noted that, whereas Tan's spiro-

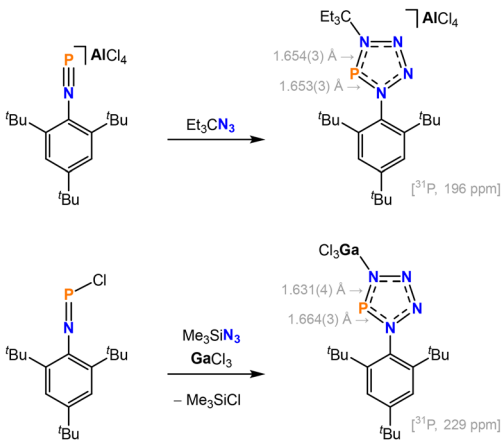

Fig. 13 Cyclization of [Mes*–N≡P]$^+$ and [Mes*–N═PCl] with azides.

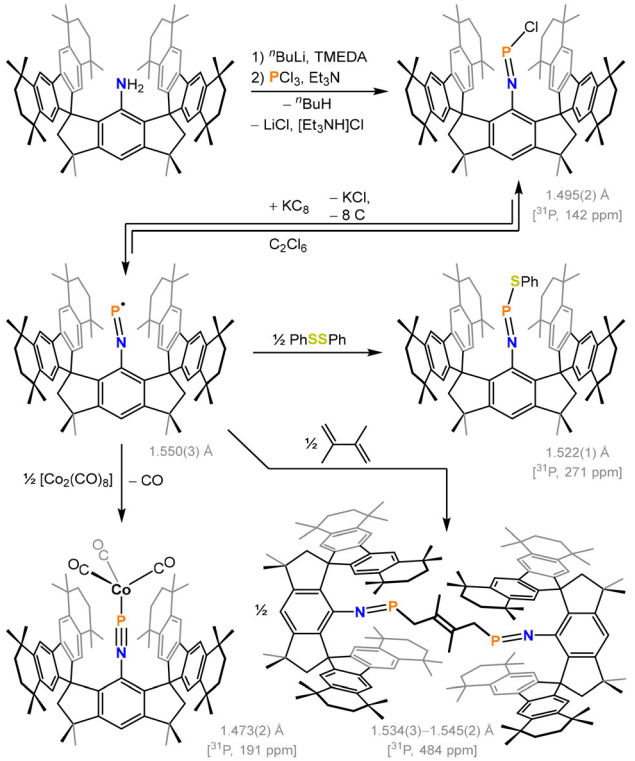

Fig. 14 Conversion of a superbulky aryl amine into an [Ar–N=PCl] motif, reduction to an [Ar–N=P]• radical, and reactivity toward PhSSPh, $[Co_2(CO)_8]$, and a conjugated diene.

fluorenyl-based [Ar–N=P]• radical is monomeric, Schulz' terphenyl-based analog, $[ArNP^{\bullet}]_2$, is a dimeric biradical.

Attempts to oxidize the [Ar–N=P]• radical with ferrocene led to activation of a cyclopentadienyl C–H bond across the N=P group, {Ar–NH-PC_5H_4}, whereas attempts to reduce the radical with KC_8 led to insertion of the P-atom into one spirofluorenyl group. Other significant reactivity patterns of [Ar–N=P]• include {P–Co} and {P–S} bond formation with $[Co_2(CO)_8]$ and PhSSPh, which act as sources of the radical fragments, $[Co(CO)_4]^{\bullet}$ and PhS•, respectively. Furthermore, reaction with a conjugated diene did not lead to a Diels–Alder cyclization product, but instead generated P–C bonds at the 1,4-positions of the diene.

An aryl-stabilized As≡N derivative

As indicated by the enthalpic data in Fig. 5, the chemistry of As≡N adducts should be much more constrained than the chemistry of P≡N adducts, and as expected, the literature on this 4p–2p diatomic is comparatively limited.

By sequentially treating Mes*-NH_2 with $AsCl_3$, ^{n}BuLi, and Et_3N, Burford could generate an $\{As_2N_2\}$ fragment in the cyclic species, $[Mes^*–NAsCl]_2$, (Fig. 15).[69] Notably, the crystalline iminoarsine is dimeric in contrast to its phosphorus congener (Fig. 6), although it is likely in equilibrium with monomeric [Mes*–N=AsCl] in solution. In a subsequent study, Schulz found that treating a solution of $[Mes^*–NAsCl]_2$ with $GaCl_3$ led to formation of the triple-bonded species, $[Mes^*–N{\equiv}As][GaCl_4]$.[70]

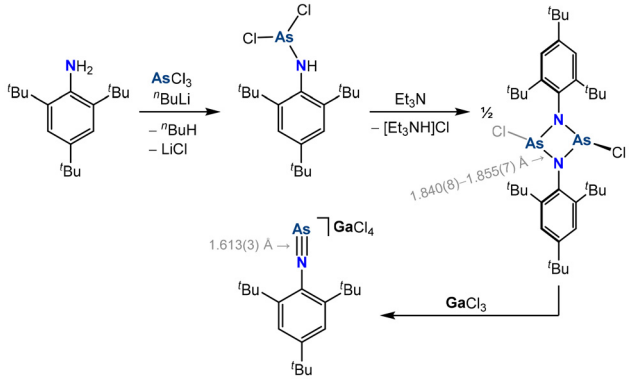

Fig. 15 Synthesis of [Mes*–N≡As][$GaCl_4$].

The $[Mes^*–N{\equiv}As]^+$ ion undergoes [3 + 2] cycloaddition with Ph_3CN_3 to form a cationic and disubstituted tetrazarsole, $[Mes^*(N_4As)CPh_3][GaCl_4]$, whereas Me_3SiN_3 affords a $GaCl_3$ adduct, $[Mes^*(N_4As)GaCl_3]$ (Fig. 16).[70,71] Interestingly, the trityl salt is unstable and cleanly eliminates Ph_3CCl while forming the $GaCl_3$ adduct.

Aryl-stabilized Sb≡N and Bi≡N synthons

Whereas Sb≡N and Bi≡N linkages have hitherto not been isolated in stable, crystallographically characterized molecules, these triple-bonded fragments have been implicated as intermediates *en route* to dimeric forms of the interpnictogen motifs. By treating the amino(dichloro)stibine, [Mes*–N($SiMe_3$)–$SbCl_2$] with two equivalents of silver triflate, Schulz isolated the thermally unstable derivative, [Mes*–N($SiMe_3$)–Sb(O_3SCF_3)$_2$].[72] This triflate species eliminated $Me_3SiO_3SCF_3$ to form a transient [Mes*–N≡Sb](SO_3CF_3) intermediate, which dimerized to form a cyclic $\{Sb_2N_2\}$ motif, $[Mes^*–NSb(O_3SCF_3)]_2$ (Fig. 17).[69]

Another example of the propensity for antimony and bismuth to form four-membered $\{Sb_2N_2\}$ and $\{Bi_2N_2\}$ rings rather than triple-bonded species such as the hypothetical molecules, "[Ar–N≡Sb](SO_3CF_3)" or "[Ar–N≡Bi](SO_3CF_3)", was reported by Schulz (Ar = 2,6-(2,4-6-$Me_3C_6H_2$)$_2C_6H_3$). Upon exposing the cyclic chloride precursors, $[Ar–NSbCl]_2$ or $[Ar–NBiCl]_2$, to two equivalents of silver triflate, the cyclic $\{Sb_2N_2\}$ and $\{Bi_2N_2\}$ structures remained intact, instead of undergoing retro [2 + 2] cyclization (Fig. 18).[73]

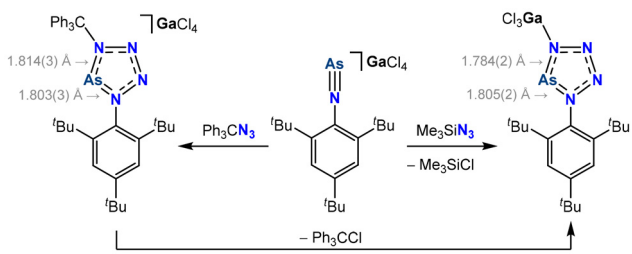

Fig. 16 Cyclization of [Mes*–N≡As][$GaCl_4$] with azides.

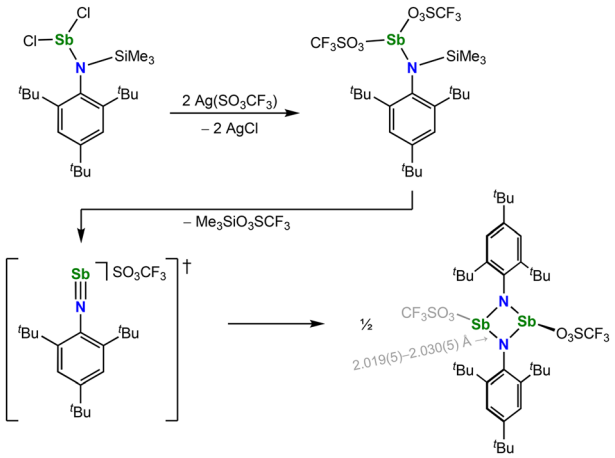

Fig. 17 Elimination of $Me_3SiO_3SCF_3$ from an aminobis(triflato)stibine to form a transient Sb≡N linkage.

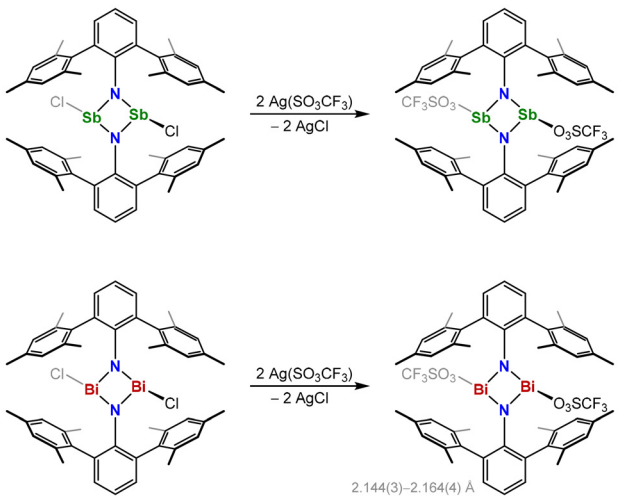

Fig. 18 Dimeric structures of the terphenyl-stabilized triflates, [ArNSb] (SO_3CF_3) and [ArNBi](SO_3CF_3).

When stirred with sodium azide in THF, $[Mes^*–NSbCl]_2$ undergoes halide exchange with NaN_3 to form the azide derivative, $[Mes^*–NSb(N_3)]_2$, which retains its four-membered $\{Sb_2N_2\}$ core. The choice of NaN_3 proved critical to this transformation, given that an azide reagent such as Me_3SiN_3 did not affect any halide exchange, whereas AgN_3 led to a more complicated transformation also involving insertion of a C–H bond from a ^{t}Bu group across the N–Sb linkage (Fig. 19). Treatment of $[Mes^*–NSb(N_3)]_2$ with a bulky Lewis acid such as $B(C_6F_5)_3$ led to reactivity characteristic of a monomeric Sb≡N fragment, undergoing a [3 + 2] cycloaddition with the azide, to form a tetrazastibole motif such as $[Mes^*(N_4Sb)(B(C_6F_5)_3)]$, which is thermally stable up to 160 °C.[74]

Carbene-stabilized P≡N systems

Various combinations of N-heterocyclic carbenes (NHC) and cyclic alkyl amino carbene (CAAC) have been installed as

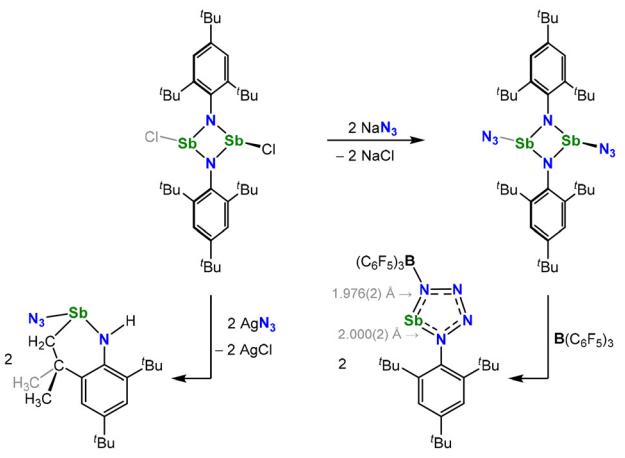

Fig. 19 Ring-opening of an azide-substituted $\{N_sSb_2\}$ heterocycle, followed by cyclization between azide and a formal Sb≡N moiety.

capping groups on two-coordinate P≡N and As≡N motifs. The π-bonds of the resulting adducts are delocalized across the dipnictogen and carbene moieties, thereby stabilizing the interpnictogen fragments but also lowering their bond order, such that the weight of an {L–E≡N–L} resonance contributor is diminished.

In 2010, Bertrand reported a P≡N adduct stabilized between an N-heterocyclic carbene and a cyclic alkyl amino carbene (Fig. 20).[75] The synthesis commences with oxidation of an NHC with Br_2 followed by reaction with ammonium hydroxide to form a guanidine fragment. Subsequent deprotonation with ^{n}BuLi and treatment with PCl_3 generated an $[(NHC)N–PCl_2]$ intermediate; further reaction with a CAAC ligand, followed by reduction with magnesium afforded the

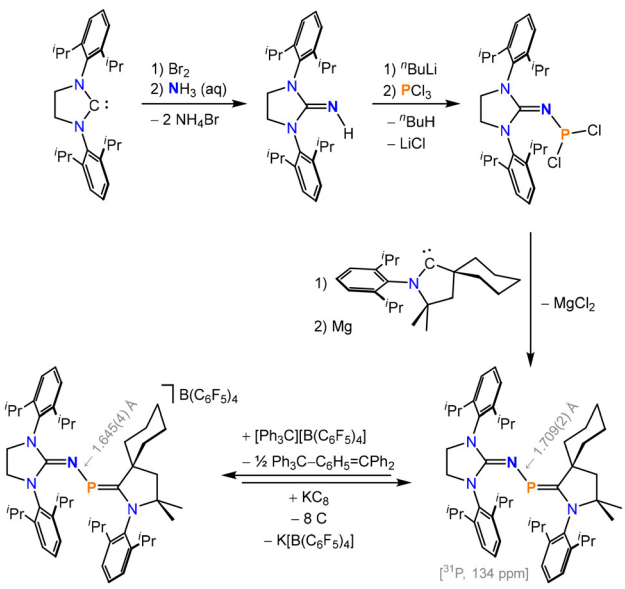

Fig. 20 Construction of a P≡N fragment stabilized by NHC and CAAC type ligands, along with its oxidation to a radical cation.

neutral [(NHC)N–P(CAAC)] adduct. Remarkably, the carbene-stabilized P≡N adduct is stable toward air, both in the solid state and in solution. Moreover, oxidation with $[Ph_3C][B(C_6F_5)_4]$ generates a radical cation, $[(NHC)N–P(CAAC)]^{\bullet+}$, with significant spin-density on phosphorus, given its ^{31}P hyperfine coupling observed by X-band EPR.

An NHC ligand may also be combined with other types of neutral ligand, for stabilizing an adduct of P≡N. Vidović showed how a silyl guanidine would react with PCl_3 to form an $[(NHC)N–PCl_2]$ intermediate, which would further react with Ramirez' carbodiphosphorane,[76] Ph_3PCPPh_3. The resulting chloride salt, $[(NHC)N–PCl–C(PPh_3)_2]Cl$ could subsequently have its halides abstracted using $AgSbF_6$ to yield an $[(NHC)N{=}P–C(PPh_3)_2](SbF_6)_2$ salt (Fig. 21).[77] Considering that the dicationic fragment contains P≡N coordinated by two neutral ligands, it represents a doubly oxidized analog of Bertrand's [(NHC)N–P(CAAC)] system (Fig. 20). In accord, the P–N bond distance in the dicationic species is considerably shorter than that in Bertrand's neutral analog (by 0.115 Å), and the phosphorus nucleus is significantly more deshielded (410 ppm *vs.* 134 ppm).

The free P≡N molecule trimerizes even under cryogenic conditions (25 K, Fig. 2) and decomposes further to polymeric products at higher temperature. By treating a CAAC, capped with a silylimino group, with a silylated trichlorophosphoraneimine, LaPierre isolated a $[(CAAC)NPCl_2NSiMe_3]$ motif. This {NPN} synthon could react further with PCl_3 and then another equivalent of CAAC to afford a $[(CAAC)NPCl_2NPCl(CAAC)]Cl$ salt. Whereas this chlorinated {NPNP} synthon proved difficult to reduce in a clean fashion with reagents such as KC_8, Zn, and Mg, it could be smoothly converted with metallic manganese into a head-to-tail dimer of P≡N, namely [(CAAC)NPNP(CAAC)] (Fig. 22).[78] The LUMO of this species possesses a large amplitude on the central phosphorus atom of the {NPNP} spine. Considering that reduction would generate a radical species, treatment of [(CAAC)NPNP(CAAC)] with KC_8 led to dimerization, forming a P–P coupled product coordinated by two K^+ ions. The study also demonstrated how analogous NHC-based systems, [(NHC)NPNP(NHC)], could be prepared; these were subjected to one-electron oxidation with

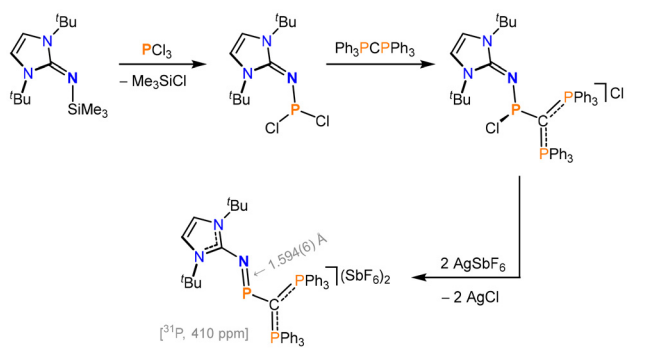

Fig. 21 A dicationic adduct of P≡N stabilized by an NHC ligand and a carbodiphosphorane.

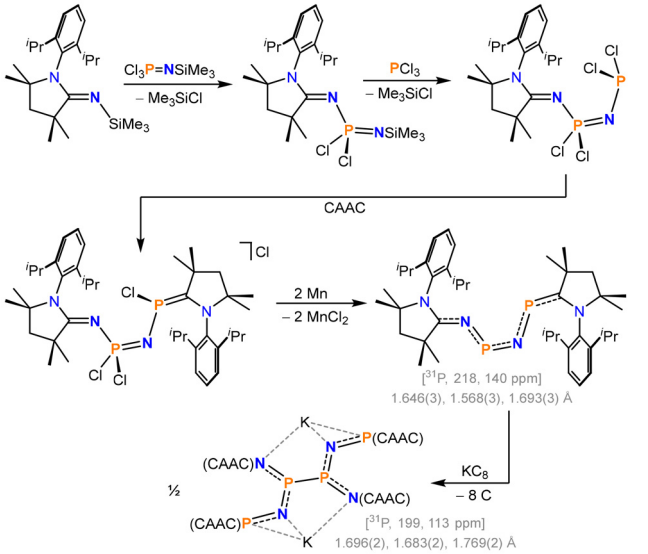

Fig. 22 Synthesis and reductive coupling of a CAAC-stabilized head-to-tail dimer of P≡N.

$[FeCp_2][SbF_6]$, forming monomeric cation radicals, [(NHC)NPNP(NHC)][SbF_6].

A carbene-stabilized As≡N system

In 2020, Tamm showed how a silyl guanidine, comprising an imido functionality and an N-heterocyclic carbene fragment, would react with $AsCl_3$ with elimination of Me_3SiCl (Fig. 23).[79] Subsequent coordination of an NHC-type carbene, followed by reduction using two equivalents of KC_8, generated an adduct of As≡N bearing two different NHC ligands. The presence of 2,6-diisopropylphenyl substituents in one NHC moiety and mesityl groups in the other resulted in a system devoid of positional crystallographic disorder within the central As≡N unit.

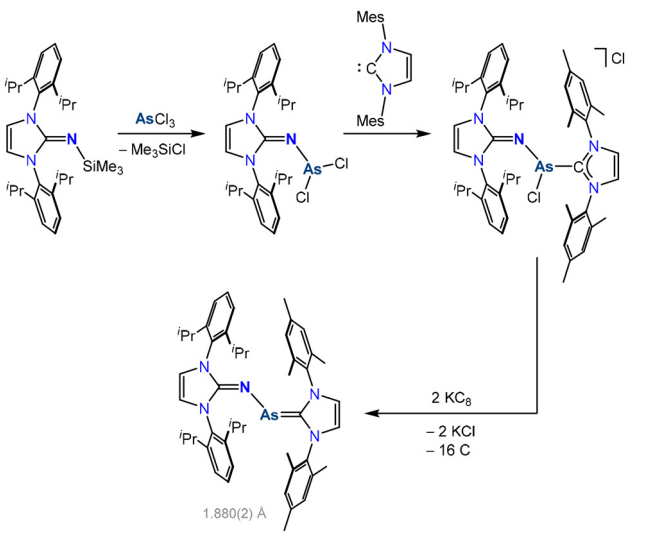

Fig. 23 Synthesis of an As≡N adduct stabilized using NHC ligands.

The analogous phosphorus mononitride adduct, [(NHC)P–N(NHC)] was also isolated in the same study, following a similar synthetic protocol.

Arene- and alkene-stabilized P≡N systems

Some adducts of P≡N have been stabilized using arene or diene-type ligands. In principle, such compounds could be envisaged to afford the free diatomic molecule upon elimination of the unsaturated organic fragment.

Cummins showed how the lithium amide, [**A**NLi(OEt$_2$)] (**A** = $C_{14}H_{10}$ or anthracene[80]), would react with PCl_3 to form an [**A**NPCl_2] motif, containing a doubly chlorinated P≡N motif (Fig. 24).[81] Further reduction using magnesium anthracenide [**A**Mg(THF)$_3$] afforded a P–N linkage stabilized between two anthracene moieties. This anthracene-sandwiched species, [**A**P–N**A**], decomposes at 95 °C in C_6D_6 solution, leading to NMR resonances from free anthracene as well as a pale yellow solid. The latter result hints that it might be possible to transfer P≡N in solution.

Leveraging the silylated chlorophosphine, [$(Me_3Si)_2$N–PCl_2], Schulz showed how sequential expulsion of two equivalents of Me_3SiCl may deliver a disguised form of P≡N.[82] Elimination of the first equivalent of Me_3SiCl and trapping with 2,3-dimethylbutadiene generated a Diels–Alder cyclization intermediate, [$(Me_3SiNPCl)(CH_2CMeCMeCH_2)$]. Elimination of a second equivalent of Me_3SiCl led to tetramerization into an eight-membered ring, having alternating P and N atoms, [$(PN)_4(CH_2CMeCMeCH_2)_4$] (Fig. 25). This tetrameric structure contrasts with the six-membered triphosphazene structure formed when free P≡N oligomerizes at 25 K (Fig. 2). The tetrameric species also showed utility as a ligand; on refluxing with [$Mo(CO)_6$], a facial, phosphorus-ligated complex, [$Mo(CO)_3${$(PN)_4(CH_2CMeCMeCH_2)_4$}], was isolated.

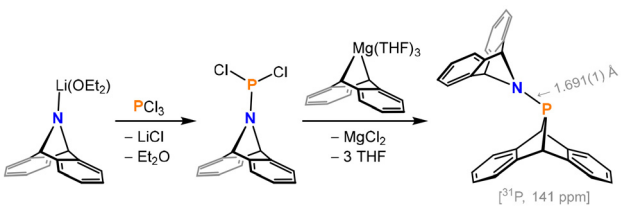

Fig. 24 Assembly of a P≡N adduct within a bis(anthracene) framework.

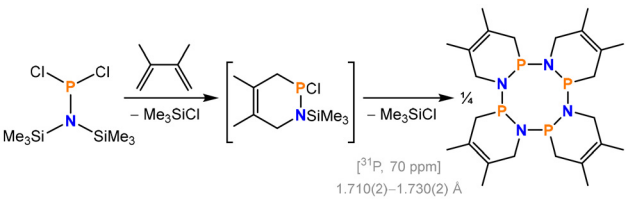

Fig. 25 Stepwise elimination of Me_3SiCl from [$(Me_3Si)_2$N–PCl_2], and trapping with a butadiene, leading to a tetrameric Diels–Alder adduct of P≡N.

E≡N diatomics stabilized by transition metal fragments

Metal fragments can be used to stabilize diatomic E≡N motifs as substituent-free ligand groups. The stability of these motifs relies on cooperative σ-donation from the E≡N ligand to an empty metal d-orbital as well as backdonation from the metal to the antibonding π-manifold of the E≡N ligand. Such donor–acceptor interactions enable electronic tunability of the redox state of the two-atom ligand; furthermore, postsynthetic release of (functionalized) E≡N fragment could enable the metal nodes to act essentially as protective groups for controlled reactivity studies of the interpnictogens.

In 2016, Cummins showed how the terminal vanadium nitride, Na[{Xyl(^{t}Bu)N}$_3$V≡N],[83] could react with the anthracene-scaffolded chlorophosphine, [**A**PCl],[84] to form an unobserved P–N linked intermediate, [{Xyl(^{t}Bu)N}$_3$V≡N–P**A**] (which was later isolated in an independent study[85]). Subsequent release of anthracene led to a putative, monomeric vanadium(III) complex, [{Xyl(^{t}Bu)N}$_3$V–N≡P], which rapidly trimerized to form a *cyclo*-P_3 core, [({Xyl(^{t}Bu)N}$_3$V≡N)$_3$(P_3)] (Fig. 26).[86]

The intermediacy of a monomeric [{Xyl(^{t}Bu)N}$_3$V–N≡P] complex could be probed through trapping with 1,8-naphthalene disulfide, {$C_{10}H_6S_2$}, resulting in a net oxidative addition at phosphorus, [{Xyl(^{t}Bu)N}$_3$V≡N–P{$S_2C_{10}H_6$}]. The trimeric species, [({Xyl(^{t}Bu)N}$_3$V≡N)$_3$(P_3)], also displays reactivity characteristic of a monomeric P≡N complex, forming phosphacyclopropane and phosphacyclopropene motifs with 4-octene and $Me_3SiC{\equiv}CSiMe_3$, respectively, in a thermally reversible manner. Moreover, thermolysis of the trimer, [({Xyl(^{t}Bu)N}$_3$V≡N)$_3$(P_3)], led to a dimeric disphosphene motif, [{Xyl(^{t}Bu)N}$_3$V≡N–P=P–N≡V{N(^{t}Bu)Mes}$_3$].

In 2020, Smith isolated the first example of a stable, monomeric P≡N complex.[87] Coupling of the mono-atomic ligands in an iron(IV) nitride complex, [{PhB(^{i}Pr$_2$Im)$_3$}Fe≡N],[88] and a molybdenum(VI) phosphide complex, [{N($CH_2CH_2NSiMe_3$)$_3$}Mo≡P],[89,90] resulted in a linear {Mo^{II}–P≡N–Fe^{II}} motif, containing a high-spin, S = 2 iron(II) center (Fig. 27). When treated with three equivalents of *tert*-butyl isocyanide, the dinuclear P≡N complex dissociated to a bimetallic salt, having a terminal, phosphorus-bound P≡N ligand coordinated to molybdenum, [{PhB(^{i}Pr$_2$Im)$_3$}Fe(CN^tBu)$_3$][{N($CH_2CH_2NSiMe_3$)$_3$}Mo–P≡N]. Interestingly, crystals of the {Mo–P≡N} complex could be photolyzed to afford the thermodynamically more stable linkage isomer, [{N($CH_2CH_2NSiMe_3$)$_3$}Mo–N≡P]$^-$. Based on the elongation of the P≡N bond (0.055 Å), the photolytically generated, nitrogen-bound N≡P ligand appears to be a stronger π-acceptor ligand than its phosphorus-bound isomer. Moreover, the energy of a side-on bound phosphorus mononitride motif, {Mo(η^2-PN)}, was computed to lie more than 40 kcal mol^{-1} above the nitrogen-bound N≡P isomer, in line with a very high thermal barrier for interconversion.

The reactivity of the molybdenum-bound P≡N ligand is in keeping with a triple-bonded resonance form. Thus, metalation using a rhodium(I) PPP-pincer complex led to extrusion of the

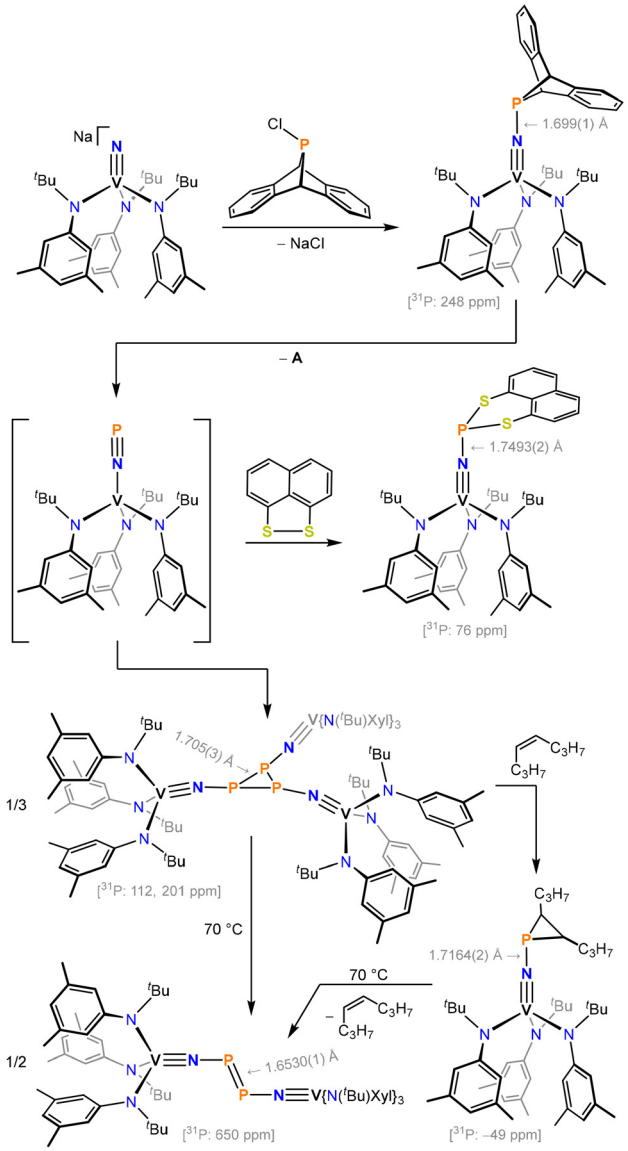

Fig. 26 P-atom transfer to a terminal vanadium nitride, forming a transient P≡N complex, along with its trimerization, oxidation and [2 + 1] cyclization chemistry.

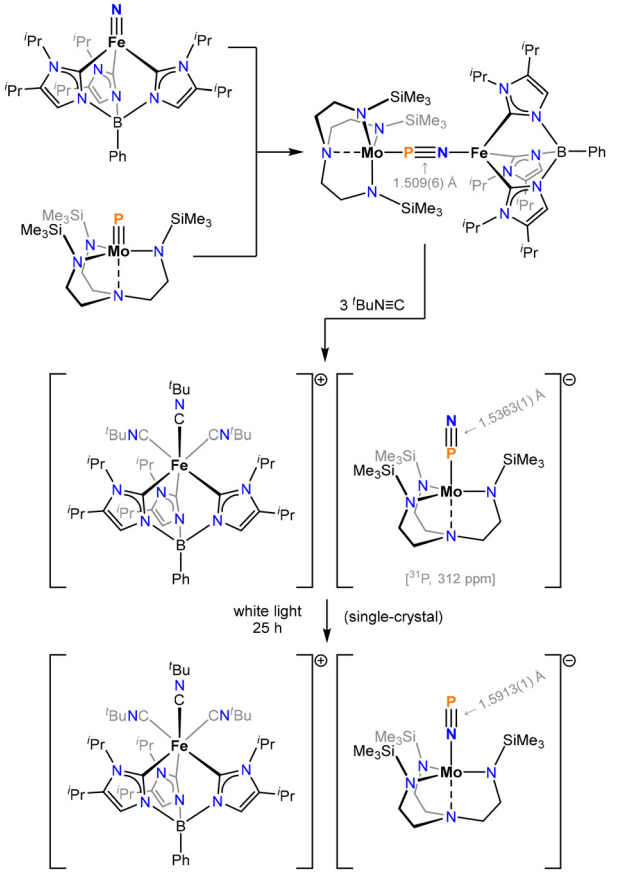

Fig. 27 Coupling of atomic ligands, {Fe≡N} and {Mo≡P}, to dinuclear P≡N complex; dissociation into a mononuclear {Mo–P≡N} complex, and photolytic linkage isomerism.

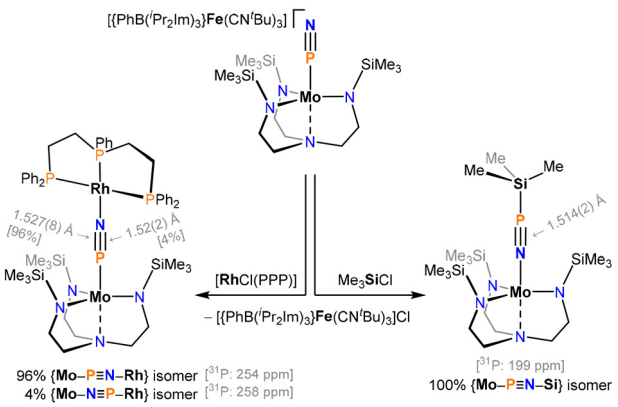

Fig. 28 Functionalization of a {Mo–P≡N} complex with Rh^{I} and silyl fragments.

iron(II) salt, $[\{PhB(^{i}Pr_2Im)_3\}Fe(CN^{t}Bu)_3]Cl$, along with formation of a linear {Mo–P≡N–Rh} fragment (Fig. 28). The crystal structure revealed 96% of the {Mo–P≡N–Rh} linkage isomer, along with a minor component corresponding to 4% of a {Mo–N≡P–Rh} structure. In a similar fashion, silylation with Me_3SiCl afforded a linearly coordinated complex, $[\{N(CH_2CH_2NSiMe_3)_3\}Mo–P{\equiv}N–SiMe_3]$ as a single linkage isomer. It is notable that the molybdenum-bound P≡N ligand can be silylated, given that elimination of Me_3SiCl is a critical step in the formation of a range of the organic P≡N derivatives (see previous sections, Fig. 7, 22 and 25). Accordingly, the molybdenum center seems to enhance the nucleophilicity of the P≡N ligand.

In 2022, Cummins demonstrated transfer of P≡N in solution. When subjecting chlorophosphine, [APCl], to halide metathesis with NaN_3 in THF (using LiCl as phase-transfer catalyst), a thermally unstable azido derivative, [APN_3], formed.[91] In a molecular beam mass spectrometry experiment (42 °C), the [APN_3] species showed release of *m*/*z* fragments corresponding to N_2, P≡N, and anthracene (Fig. 29). On a bulk sample, decomposition occurred with explosion at 68 °C.

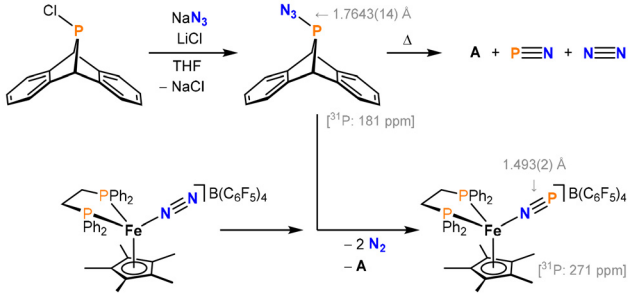

Fig. 29 Formation of anthracene-scaffolded azidophosphine along with transfer of P≡N to Fe^{II} complex.

The release of free P≡N enabled [APN_3] to be used as a P≡N transfer vehicle; exposing the iron(II) dinitrogen precursor, [(dppe)Cp*Fe–N≡N][$B(C_6F_5)_4$], to [APN_3] led to the smooth formation of P≡N complex, [(dppe)Cp*Fe–N≡P][$B(C_6F_5)_4$]. It is remarkable that in this coordination sequence, the [APN_3] reactant imposes very limited structural preorganization to favor a specific isomer; nevertheless the nitrogen-bound P≡N complex forms selectively in the solution transfer protocol.

In 2025, our group showed how an electrophilic osmium(VI) nitride cation and phosphaethynolate[92–94] undergo N–P coupling, expel CO, and form a P≡N ligand coordinated to osmium(II) (Fig. 30).[95] Whereas Na(OCP) is often regarded as a two-electron oxidant in phosphorus atom transfer reactions, the changes in oxidation state for osmium suggest that, in our case, Na(OCP) may be considered a four-electron reductant.

The reactivity of the {Os–N≡P} complex is strongly influenced by the efficient backdonation from the Os^{II} ion. Upon reaction with elemental sulfur, the phosphorus center associates with two sulfur atoms, forming a trigonal planar $[NPS_2]^{2-}$ fragment. Notably, this two-fold oxidation necessitates that the osmium center provides two electrons when the P≡N moiety converts into the new ligand fragment. In another oxidative conversion, the Os^{II}-coordinated P≡N ligand could be chlorinated with Ph_3CCl to form an $[NPCl]^-$ fragment bound to Os^{III}. This paramagnetic complex could be converted with Me_3SiN_3 to form an aromatic $[PN_4]^-$ ligand motif. Attempts to reduce this paramagnetic Os^{III} species did not furnish a diamagnetic Os^{II} derivative but instead led to a retro [3 + 2] cycloaddition, regenerating the P≡N ligand (Fig. 31).

Whereas the aforementioned coupling schemes based on metal–ligand multiple bonds have generated substituent-free

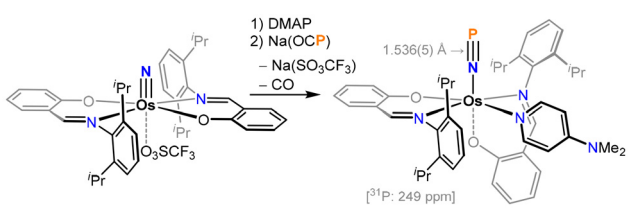

Fig. 30 Phosphorus-atom transfer from Na(OCP) to an {Os^{VI}≡N} functionality to form an {Os^{II}–N≡P} complex.

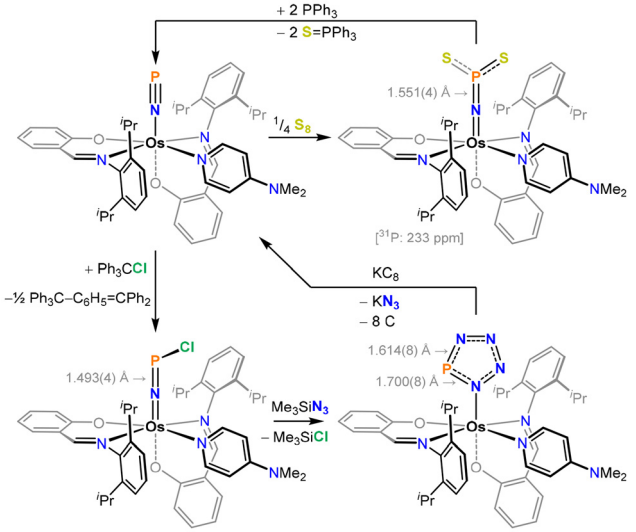

Fig. 31 Reactivity of an {Os–N≡P} complex, including oxidation with sulfur and trityl chloride, as well as cyclization with azide.

P≡N ligands, there are also notable examples generating the diatomic fragment with an appended organic or main-group fragment. For example, in 1995, Cummins reported how the terminal molybdenum phosphide complex, [{Xyl(^{t}Bu)N}$_3$Mo≡P], reacts with mesityl azide to form a [{Xyl(^{t}Bu)N}$_3$Mo–P≡N–Mes] complex (Fig. 32).[96] The structural similarity of this complex to Smith's molybdenum-bound P≡N derivatives (Fig. 27 and 28) is striking.

More recently, Tilley treated an NHC-stabilized ruthenium(II) precursor, [(NHC)Cp*RuCl] with Na(OCP), resulting in an initial halide metathesis step. Given the d^6 electronic configuration of ruthenium, this protocol did not form an electronically stable, terminal {Ru≡P} functionality, but instead led to P-atom insertion into of one of the aryl groups of the NHC ligand, along with dearomatization and formation of a phosphanorcaradiene motif (Fig. 33). It was found that this complex reacts as a masked ruthenium phosphinidene. Thus, when treated with tosyl azide, deazotation along with P–N coupling led to a [(NHC)Cp*Ru–P≡N–$SO_2C_6H_4Me$] complex.[97] The structural similarity between Tilley's {Ru–P≡N–SO_2Ar}

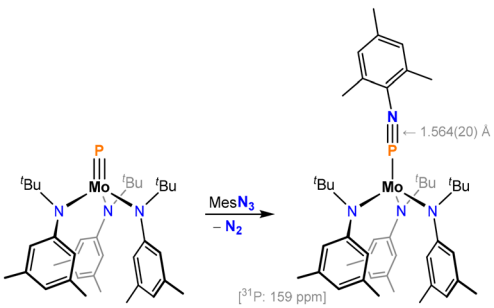

Fig. 32 Coupling of a terminal molybdenum phosphide with mesityl azide to form a $[P{\equiv}N{-}Mes]^+$ ligand.

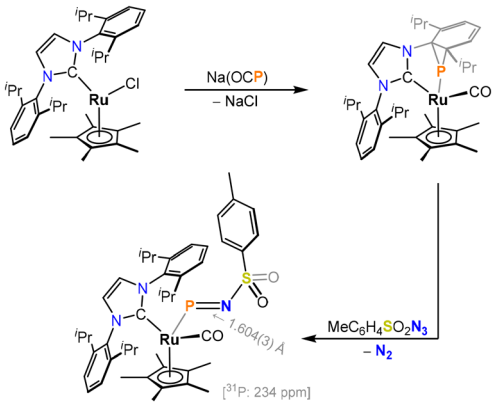

Fig. 33 Coupling of tosyl azide with a phosphanorcaradiene complex, leading to a ruthenium-bound $[P{=}N{-}SO_2C_6H_4Me]^-$ ligand.

core and Niecke's isoelectronic {Fe–P═N–Ar} complex (Fig. 10) is noteworthy.

Conclusions and outlook

Whereas the dinitrogen molecule has been known for more than 250 years, and is considered to possess one of the strongest possible triple bonds, the heavier group 15 elements are not anywhere near as efficient at forming stable π-bonded motifs. The chemistry of these fascinating, orbitally mismatched triple bond systems has largely remained dormant. In the present perspective, we have surveyed the chemistry of interpnictogen motifs, E≡N, consisting of phosphorus, arsenic, antimony, or bismuth (E) with a triple bond to nitrogen. The first member of this family, P≡N, was already prepared nearly a century ago, whereas the last member of the series, Bi≡N, was not reported until 1993. Studies of the free E≡N diatomics have essentially been limited to high-temperature, gas-phase experimentation, allowing highly accurate data on dissociation enthalpies, stretching frequencies, and bond distances, but also preventing all but the simplest reactivity studies to be pursued. In the case of phosphorus mononitride, the gaseous diatomic has further been trapped in cryogenic noble gas matrices, enabling fundamental reactivity studies of the P≡N triple bond, albeit on a submolar scale.

Whereas the full series of pnictogen-nitrogen triple bonds, P≡N, As≡N, Sb≡N, through Bi≡N has been established in the gas-phase, the viability of these motifs in molecular form has only been verified for P≡N, and to a very limited extent, As≡N. In 1988, Niecke made the first groundbreaking discovery in the quest to incorporate E≡N triple-bonds in isolable molecules. Starting from a bulky aniline and phosphorus trichloride, an elimination strategy led to the assembly of the multiple-bonded species, [Mes*–N═PCl] and $[Mes^*{-}N{\equiv}P]^+$. These supermesityl scaffolds have now become a mainstay in synthetic p-block and d-block chemistry. Given the positive charge of $[Mes^*{-}N{\equiv}P]^+$ – or the easily displaced chloride group in [Mes*–N═PCl] – these interpnictogen systems display distinct electrophilic reactivity patterns. Notable topics include the synthesis of carbon-free aromatics, coordination of Lewis bases, hypercoordinated and multiple-bonded phosphorus(III) and phosphorus(V) motifs, transition metal coordination, and the extension of these reaction types to encompass the As≡N triple bond. Very recently, Tan introduced a superbulky spirofluorenyl-encased aryl system as a second-generation scaffold for P≡N triple-bond chemistry, opening new vistas in radical transformations of a formally mono-anionic form of phosphorus mononitride, $[P{=}N]^{\bullet-}$. Going forward, such super bulky aryl scaffolds hold much promise for isolation of the most elusive E≡N triple bonds, and fleeting derivatives, given their ability to kinetically suppress undesirable degradation pathways, proceeding through dimerization and/or bond activation steps.

In 2010, Bertrand reported the first neutral ligand adduct of P≡N, utilizing NHC and CAAC type ligands to stabilize a remarkably stable [(NHC)N–P(CAAC)] motif. While such system is redox active, chemical reactions of its {PN} core are limited by the steric encumbrance of the carbene ligands. Further carbene-based methodologies involve the genesis of linear {PNPN} motifs as well as a rare example of an {AsN} adduct. In addition, P≡N has been sandwiched between anthracene fragments, and a Diels–Alder cyclization protocol has even enabled isolation of a cyclic tetrameric form of the diatomic molecule. Looking beyond the current state of art, stabilization strategies based upon carbodiphosphorane ligands or frustrated Lewis pairs may gain traction as stabilizing groups for E≡N chemistry, considering their recent deployment for stabilizing homoatomic As_2, Sb_2, and Bi_2 motifs.[98,99]

The final frontier in E≡N chemistry is coordination to transition metal centers. In 2020, Smith isolated the first complex containing a diatomic P≡N ligand, and in 2022, Cummins demonstrated a solution transfer of P≡N from an organic scaffold onto an iron(II) complex. Metal complexes bearing P≡N ligands display unique chemistry, including photoisomerization, dissociation/association reactions toward other metal fragments, atom transfer and cyclization reactivity. Functionalized P≡N ligands ($R{-}N{\equiv}P^+$, $R{-}N{=}P^-$) even display linear *versus* bent coordination modes, in analogy to NO ligands in nitrosyl complexes. Strikingly, the ability of electron-rich metal centers to backdonate may render coordinated P≡N ligands nucleophilic, up to the point where their electronic structure is best described as $[P{=}N]^{2-}$. This nucleophilicity should be seen against the backdrop of the more electrophilic reactivity of derivatives such as $[Mes^*{-}N{=}P]^+$, hence defining two distinctive reactivity paradigms for organic adducts and transition metal complexes of P≡N. Considering the strong enthalpic stabilization from π-backdonating interactions between a metal center and an E≡N diatomic ligand, it seems plausible that metal-based strategies may hold the key to isolating the heaviest members of interpnictogen diatomics, E≡N.

Overall, this perspective has outlined how the molecular chemistry of the rare P≡N motif keeps growing, while the chemistry of As≡N remains extremely limited, and systems based on Sb≡N and Bi≡N are virtually beyond reach. From

enthalpic considerations, the thermodynamic instability of E≡N diatomics is not solely rooted in the moderate strength of the interpnictogen triple bonds, but also in the abnormally high stability of the N≡N triple bond that forms when the E≡N unit ruptures, and the elements recombine. The pnictogen mononitrides are therefore likely to be the thermodynamically most challenging interpnictogen triple-bond motifs that may be pursued.

Author contributions

This perspective was written through the contributions of all authors.

Conflicts of interest

There are no conflicts to declare.

Abbreviations

A	$C_{14}H_{10}$ or anthracene
Ar	Various aryl groups
bipy	2,2′-Bipyridine
^{n}Bu	normal-Butyl
^{t}Bu	*tert*-Butyl
CAAC	Various cyclic alkyl amino carbenes
Cp	Cyclopentadienyl
Cp*	Pentamethylcyclopentadienyl
dppe	1,2-Bis(diphenylphosphino)ethane
Et	Ethyl
Im	Imidazole
Mes	2,4,6-$Me_3C_6H_2$ (mesityl)
Mes*	2,4,6-$^{t}Bu_3C_6H_2$ (supermesityl)
Me	Methyl
nacnac$^-$	$\{CH_3(C{=}NAr)CH(C{=}NAr)CH_3\}^-$ (Ar = 2,6-$^{i}Pr_2C_6H_3$)
NHC	Various N-heterocyclic carbenes
Ph	Phenyl
^{i}Pr	iso-propyl
TMEDA	Tetramethylethylenediamine
Xyl	3,5-$Me_2C_6H_3$ (xylyl)

Data availability

This perspective reports no primary research data.

Acknowledgements

We thank The Carl Trygger Foundation (CTS 23:2945 and CTS 25:4604), The Swedish Research Council (2022-03154), and The Crafoord Foundation (20230776 and 20250783) for funding.

References

1 J. G. Chen, R. M. Crooks, L. C. Seefeldt, K. L. Bren, R. M. Bullock, M. Y. Darensbourg, P. L. Holland, B. Hoffman, M. J. Janik, A. K. Jones, M. G. Kanatzidis, P. King, K. M. Lancaster, S. V. Lymar, P. Pfromm, W. F. Schneider and R. R. Schrock, *Science*, 2018, **360**, eaar6611.
2 J. Priestley, *Philos. Trans. R. Soc.*, 1772, **62**, 147–264.
3 M. E. Weeks, *J. Chem. Educ.*, 1932, **9**, 215.
4 J. Curry, L. Herzberg and G. Herzberg, *J. Chem. Phys.*, 1933, **1**, 749.
5 J. W. T. Spinks, *Z. Phys.*, 1934, **88**, 511–514.
6 N. H. Coy and H. Sponer, *Phys. Rev.*, 1940, **58**, 709–713.
7 O. Shestakov and E. H. Fink, *Chem. Phys. Lett.*, 1993, **211**, 473–477.
8 B. E. Turner and J. Bally, *Astrophys. J.*, 1987, **321**, L75–L79.
9 L. M. Ziurys, *Astrophys. J.*, 1987, **321**, L81.
10 V. M. Rivilla, M. N. Drozdovskaya, K. Altwegg, P. Caselli, M. T. Beltrán, F. Fontani, F. F. S. van der Tak, R. Cesaroni, A. Vasyunin, M. Rubin, F. Lique, S. Marinakis, L. Testi, H. Balsiger, J. J. Berthelier, J. De Keyser, B. Fiethe, S. A. Fuselier, S. Gasc, T. I. Gombosi, T. Sémon and C.-Y. Tzou, *Mon. Not. R. Astron. Soc.*, 2020, **492**, 1180–1198.
11 L. A. Koelemay, K. R. Gold and L. M. Ziurys, *Nature*, 2023, **623**, 292–295.
12 K. P. Huber and G. Herzberg, *Molecular Spectra and Molecular Structure - IV. Constants of Diatomic Molecules*, Van Nostrand Reinhold, New York, 1979.
13 K. A. Peterson, *J. Chem. Phys.*, 2003, **119**, 11099–11112.
14 A. Jenouvrier, D. Daumont and B. Pascat, *Can. J. Phys.*, 1978, **56**, 30–44.
15 R. Breidohr, K. D. Setzer, O. Shestakov, E. H. Fink and W. Zyrnicki, *J. Mol. Spectrosc.*, 1994, **166**, 471–485.
16 R. M. Atkins and P. L. Timms, *Spectrochim. Acta, Part A*, 1977, **33**, 853–857.
17 C. Zhu, A. K. Eckhardt, A. Bergantini, S. K. Singh, P. R. Schreiner and R. I. Kaiser, *Sci. Adv.*, 2020, **6**, eaba6934.
18 C. Zhu, A. K. Eckhardt, S. Chandra, A. M. Turner, P. R. Schreiner and R. I. Kaiser, *Nat. Commun.*, 2021, **12**, 5467.
19 R. M. Atkins and P. L. Timms, *Inorg. Nulc. Chem. Lett.*, 1978, **14**, 113–115.
20 R. Ahlrichs, M. Bär, H. S. Plitt and H. Schnöckel, *Chem. Phys. Lett.*, 1989, **161**, 179–184.
21 W. Qian, R. C. Wende, P. R. Schreiner and A. Mardyukov, *Angew. Chem., Int. Ed.*, 2023, **62**, e202300761.
22 J. Jiang, L. Huang, B. Zhu, W. Fan, L. Wang, I. Y. Zhang, W. Fang, T. Trabelsi, J. S. Francisco and X. Zeng, *Angew. Chem., Int. Ed.*, 2025, **64**, e202414456.
23 J. Jiang, Y. Guo, L. Huang, L. Wang, G. Rauhut and X. Zeng, *Nat. Commun.*, 2026, **17**, 1687.
24 T. L. Henshaw, D. McElwee, D. H. Stedman and R. D. Coombe, *J. Phys. Chem.*, 1988, **92**, 4606–4610.
25 M. Ceppatelli, D. Scelta, M. Serrano-Ruiz, K. Dziubek, M. Morana, V. Svitlyk, G. Garbarino, T. Poręba,

M. Mezouar, M. Peruzzini and R. Bini, *Angew. Chem., Int. Ed.*, 2022, **61**, e202114191.
26 M. Ceppatelli, M. Serrano-Ruiz, M. Morana, K. Dziubek, D. Scelta, R. Bini and M. Peruzzini, *Acc. Chem. Res.*, 2025, **58**, 2927–2938.
27 S. Ciach and P. J. Thistlethwaite, *J. Chem. Phys.*, 1970, **53**, 3381–3382.
28 S. A. Cooke and M. C. L. Gerry, *Phys. Chem. Chem. Phys.*, 2004, **6**, 4579–4585.
29 K. Glazyrin, A. Aslandukov, A. Aslandukova, T. Fedotenko, S. Khandarkhaeva, D. Laniel, M. Bykov and L. Dubrovinsky, *Front. Chem.*, 2023, **11**, 1257942.
30 A. Schulz, in *Advances in Bismuth Chemistry*, ed. C. Lichtenberg, Springer Nature Switzerland, Cham, 2025, pp. 43–118.
31 C. Esterhuysen and G. Frenking, *Theor. Chem. Acc.*, 2004, **111**, 381–389.
32 M. V. Hopffgarten and G. Frenking, *Wiley Interdiscip. Rev.: Comput. Mol. Sci.*, 2012, **2**, 43–62.
33 P. P. Power, *Chem. Rev.*, 1999, **99**, 3463–3504.
34 P. Jerabek and G. Frenking, *Theor. Chem. Acc.*, 2014, **133**, 1447.
35 E. Niecke, M. Nieger and F. Reichert, *Angew. Chem., Int. Ed. Engl.*, 1988, **27**, 1715–1716.
36 R. Detsch, E. Niecke, M. Nieger and F. Reichert, *Chem. Ber.*, 1992, **125**, 321–330.
37 D. Gudat, H. M. Schiffner, M. Nieger, D. Stalke, A. J. Blake, H. Grondey and E. Niecke, *J. Am. Chem. Soc.*, 1992, **114**, 8857–8862.
38 E. Niecke, J. F. Nixon, P. Wenderoth, B. F. T. Passos and M. Nieger, *J. Chem. Soc., Chem. Commun.*, 1993, 846–848.
39 T. Baumgartner, D. Gudat, M. Nieger, E. Niecke and T. J. Schiffer, *J. Am. Chem. Soc.*, 1999, **121**, 5953–5960.
40 N. A. Piro, J. S. Figueroa, J. T. McKellar and C. C. Cummins, *Science*, 2006, **313**, 1276–1279.
41 P. Mayer, A. Schulz and A. Villinger, *J. Organomet. Chem.*, 2007, **692**, 2839–2842.
42 N. A. Piro and C. C. Cummins, *J. Am. Chem. Soc.*, 2008, **130**, 9524–9535.
43 M. Kuprat, M. Lehmann, A. Schulz and A. Villinger, *Inorg. Chem.*, 2011, **50**, 5784–5792.
44 A. Hinz, R. Kuzora, U. Rosenthal, A. Schulz and A. Villinger, *Chem. – Eur. J.*, 2014, **20**, 14659–14673.
45 H. Braunschweig, J. O. C. Jimenez-Halla, K. Radacki and R. Shang, *Angew. Chem., Int. Ed.*, 2016, **55**, 12673–12677.
46 B. J. Frogley, A. F. Hill, R. Shang, M. Sharma and A. C. Willis, *Chem. – Eur. J.*, 2020, **26**, 8819–8827.
47 J. Rothe, J. Bresien, F. Reiß, A. Villinger, T. Beweries and A. Schulz, *Z. Anorg. Allg. Chem.*, 2022, **648**, e202200174.
48 S. K. Milkovich, F. L. Buguis, P. D. Boyle and J. B. Gilroy, *Chem. – Eur. J.*, 2024, **30**, e202400569.
49 H. A. Spinney, N. A. Piro and C. C. Cummins, *J. Am. Chem. Soc.*, 2009, **131**, 16233–16243.
50 C. Hering, A. Schulz and A. Villinger, *Angew. Chem., Int. Ed.*, 2012, **51**, 6241–6245.
51 N. Burford, J. A. C. Clyburne, P. K. Bakshi and T. S. Cameron, *J. Am. Chem. Soc.*, 1993, **115**, 8829–8830.
52 N. Burford, J. A. C. Clyburne, P. K. Bakshi and T. S. Cameron, *Organometallics*, 1995, **14**, 1578–1585.
53 N. Burford, T. S. Cameron, D. J. LeBlanc, A. D. Phillips, T. E. Concolino, K.-C. Lam and A. L. Rheingold, *J. Am. Chem. Soc.*, 2000, **122**, 5413–5414.
54 N. Burford, H. A. Spinney, M. J. Ferguson and R. McDonald, *Chem. Commun.*, 2004, 2696–2697.
55 N. Burford, T. S. Cameron, K. N. Robertson, A. D. Phillips and H. A. Jenkins, *Chem. Commun.*, 2000, 2087–2088.
56 N. Burford, A. D. Phillips, H. A. Spinney, M. Lumsden, U. Werner-Zwanziger, M. J. Ferguson and R. McDonald, *J. Am. Chem. Soc.*, 2005, **127**, 3921–3927.
57 N. Burford, T. S. Cameron, J. A. C. Clyburne, K. Eichele, K. N. Robertson, S. Sereda, R. E. Wasylishen and W. A. Whitla, *Inorg. Chem.*, 1996, **35**, 5460–5467.
58 N. Burford, A. D. Phillips, H. A. Spinney, K. N. Robertson, T. S. Cameron and R. McDonald, *Inorg. Chem.*, 2003, **42**, 4949–4954.
59 E. Niecke, J. Hein and M. Nieger, *Organometallics*, 1989, **8**, 2290–2291.
60 D. P. Hales, T. Rajeshkumar, A. A. Shiau, G. Rao, E. T. Ouellette, R. G. Bergman, R. D. Britt, L. Maron and J. Arnold, *Inorg. Chem.*, 2024, **63**, 11296–11310.
61 E. Niecke, R. Detsch, M. Nieger, F. Reichert and W. W. Schoeller, *Bull. Soc. Chim. Fr.*, 1993, **130**, 25–31.
62 N. Burford, T. S. Cameron, K. D. Conroy, B. Ellis, M. Lumsden, C. L. B. Macdonald, R. McDonald, A. D. Phillips, P. J. Ragogna, R. W. Schurko, D. Walsh and R. E. Wasylishen, *J. Am. Chem. Soc.*, 2002, **124**, 14012–14013.
63 N. Burford, J. A. C. Clyburne, D. P. Gates, M. J. Schriver and J. F. Richardson, *J. Chem. Soc., Dalton Trans.*, 1994, 997–1001.
64 K. Huynh, C. P. Chun, A. J. Lough and I. Manners, *Dalton Trans.*, 2011, **40**, 10576–10584.
65 G. David, E. Niecke, M. Nieger, V. V. D. Gönna and W. W. Schoeller, *Chem. Ber.*, 1993, **126**, 1513–1517.
66 A. Villinger, P. Mayer and A. Schulz, *Chem. Commun.*, 2006, 1236–1238.
67 X. Wang, Y. Chen, X. Li, L. Xu and G. Tan, *J. Am. Chem. Soc.*, 2025, **147**, 36980–36986.
68 T. Beweries, R. Kuzora, U. Rosenthal, A. Schulz and A. Villinger, *Angew. Chem., Int. Ed.*, 2011, **50**, 8974–8978.
69 N. Burford, T. S. Cameron, C. L. B. Macdonald, K. N. Robertson, R. Schurko, D. Walsh, R. McDonald and R. E. Wasylishen, *Inorg. Chem.*, 2005, **44**, 8058–8064.
70 M. Kuprat, A. Schulz and A. Villinger, *Angew. Chem., Int. Ed.*, 2013, **52**, 7126–7130.
71 A. Schulz and A. Villinger, *Angew. Chem., Int. Ed.*, 2008, **47**, 603–606.
72 M. Lehmann, A. Schulz and A. Villinger, *Eur. J. Inorg. Chem.*, 2012, **2012**, 822–832.
73 M. Lehmann, A. Schulz and A. Villinger, *Angew. Chem., Int. Ed.*, 2012, **51**, 8087–8091.
74 M. Lehmann, A. Schulz and A. Villinger, *Angew. Chem., Int. Ed.*, 2011, **50**, 5221–5224.

75 R. Kinjo, B. Donnadieu and G. Bertrand, *Angew. Chem., Int. Ed.*, 2010, **49**, 5930–5933.
76 F. Ramirez, N. B. Desai, B. Hansen and N. McKelvie, *J. Am. Chem. Soc.*, 1961, **83**, 3539–3540.
77 Y. K. Loh, C. Gurnani, R. Ganguly and D. Vidović, *Inorg. Chem.*, 2015, **54**, 3087–3089.
78 E. A. LaPierre, B. O. Patrick and I. Manners, *J. Am. Chem. Soc.*, 2024, **146**, 6326–6335.
79 D. Bockfeld and M. Tamm, *Z. Anorg. Allg. Chem.*, 2020, **646**, 866–872.
80 D. J. Mindiola and C. C. Cummins, *Angew. Chem., Int. Ed.*, 1998, **37**, 945–947.
81 A. Velian and C. C. Cummins, *J. Am. Chem. Soc.*, 2012, **134**, 13978–13981.
82 C. Hering, A. Schulz and A. Villinger, *Chem. Sci.*, 2014, **5**, 1064–1073.
83 J. K. Brask, M. G. Fickes, P. Sangtrirutnugul, V. Durà-Vilà, A. L. Odom and C. C. Cummins, *Chem. Commun.*, 2001, 1676–1677.
84 A. Velian, M. Nava, M. Temprado, Y. Zhou, R. W. Field and C. C. Cummins, *J. Am. Chem. Soc.*, 2014, **136**, 13586–13589.
85 A. K. Eckhardt, M.-L. Y. Riu, P. Müller and C. C. Cummins, *Inorg. Chem.*, 2022, **61**, 1270–1274.
86 M.-A. Courtemanche, W. J. Transue and C. C. Cummins, *J. Am. Chem. Soc.*, 2016, **138**, 16220–16223.
87 J. L. Martinez, S. A. Lutz, D. M. Beagan, X. Gao, M. Pink, C.-H. Chen, V. Carta, P. Moënne-Loccoz and J. M. Smith, *ACS Cent. Sci.*, 2020, **6**, 1572–1577.
88 J. L. Martinez, H.-J. Lin, W.-T. Lee, M. Pink, C.-H. Chen, X. Gao, D. A. Dickie and J. M. Smith, *J. Am. Chem. Soc.*, 2017, **139**, 14037–14040.
89 N. C. Zanetti, R. R. Schrock and W. M. Davis, *Angew. Chem., Int. Ed. Engl.*, 1995, **34**, 2044–2046.
90 N. C. Mösch-Zanetti, R. R. Schrock, W. M. Davis, K. Wanninger, S. W. Seidel and M. B. O'Donoghue, *J. Am. Chem. Soc.*, 1997, **119**, 11037–11048.
91 A. K. Eckhardt, M.-L. Y. Riu, M. Ye, P. Müller, G. Bistoni and C. C. Cummins, *Nat. Chem.*, 2022, **14**, 928–934.
92 G. Becker, W. Schwarz, N. Seidler and M. Westerhausen, *Z. Anorg. Allg. Chem.*, 1992, **612**, 72–82.
93 D. Heift, Z. Benkő and H. Grützmacher, *Dalton Trans.*, 2014, **43**, 831–840.
94 J. M. Goicoechea and H. Grützmacher, *Angew. Chem., Int. Ed.*, 2018, **57**, 16968–16994.
95 S. Edin, C. Sandoval-Pauker, N. J. Yutronkie, Z. Takacs, F. Wilhelm, A. Rogalev, B. Pinter, K. S. Pedersen and A. Reinholdt, *Nat. Commun.*, 2025, **16**, 5596.
96 C. E. Laplaza, W. M. Davis and C. C. Cummins, *Angew. Chem., Int. Ed. Engl.*, 1995, **34**, 2042–2044.
97 T. G. Saint-Denis, T. A. Wheeler, Q. Chen, G. Balázs, N. S. Settineri, M. Scheer and T. D. Tilley, *J. Am. Chem. Soc.*, 2024, **146**, 4369–4374.
98 L. Zapf, G. Balázs, M. Scheer and E. Rivard, *Angew. Chem., Int. Ed.*, 2026, **65**, e24828.
99 P. Dabringhaus, A. Molino and R. J. Gilliard Jr, *J. Am. Chem. Soc.*, 2024, **146**, 27186–27195.

